# High Capacity, Stable Silicon/Carbon Anodes for Lithium-Ion Batteries Prepared Using Emulsion-Templated Directed Assembly

**ARTICLE** *in* ACS APPLIED MATERIALS & INTERFACES · MARCH 2014

Impact Factor: 6.72 · DOI: 10.1021/am404947z · Source: PubMed



**6 AUTHORS**, INCLUDING:

Yanjing Chen

**29** PUBLICATIONS **393** CITATIONS

SEE PROFILE

Mengyun Nie

Dalhousie University

**24** PUBLICATIONS **201** CITATIONS

SEE PROFILE

Amitesh Saha

University of Rhode Island

**12** PUBLICATIONS **48** CITATIONS

SEE PROFILE

Pradeep Guduru

Brown University

**52** PUBLICATIONS **1,522** CITATIONS

SEE PROFILE

ACS APPLIED MATERIALS & INTERFACES

Research Article

www.acsami.org

# High Capacity, Stable Silicon/Carbon Anodes for Lithium-Ion Batteries Prepared Using Emulsion-Templated Directed Assembly

Yanjing Chen,*[,†] Mengyun Nie,[‡] Brett L. Lucht,[‡] Amitesh Saha,[†] Pradeep R. Guduru,[§] and Arijit Bose*[,†]

[†]Department of Chemical Engineering [‡]Department of Chemistry, University of Rhode Island, Kingston, Rhode Island 02881, United States

[§]School of Engineering, Brown University, Providence, Rhode Island 02912, United States

**ABSTRACT:** Silicon (Si) is a promising candidate for lithium ion battery anodes because of its high theoretical capacity. However, the large volume changes during lithiation/delithiation cycles result in pulverization of Si, leading to rapid fading of capacity. Here, we report a simple fabrication technique that is designed to overcome many of the limitations that deter more widespread adoption of Si based anodes. We confine Si nanoparticles in the oil phase of an oil-in-water emulsion stabilized by carbon black (CB). These CB nanoparticles are both oil- and water-wettable. The hydrophilic/hydrophobic balance for the CB nanoparticles also causes them to form a network in the continuous aqueous phase. Upon drying this emulsion on a current collector, the CB particles located at the surfaces of the emulsion droplets form mesoporous cages that loosely encapsulate the Si particles that were in the oil. The CB particles that were in the aqueous phase form a conducting network connected to the CB cages. The space within the cages allows for Si particle expansion without transmitting stresses to the surrounding carbon network. Half-cell experiments using this Si/CB anode architecture show a specific capacity of ~1300 mAh/g Si + C and a Coulombic efficiency of 97.4% after 50 cycles. Emulsion-templating is a simple, inexpensive processing strategy that directs Si and conducts CB particles to desired spatial locations for superior performance of anodes in lithium ion batteries.

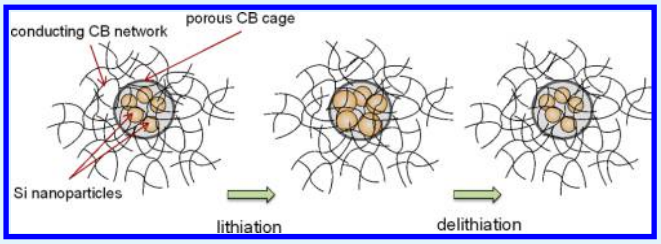


**KEYWORDS:** *emulsion templating, silicon/carbon anode, directed assembly*

## 1. INTRODUCTION

Lithium ion batteries (LIB) for future electric vehicles and portable electronics must have high capacity and charge/discharge stability over a large number of cycles. Silicon (Si) has a high specific theoretical capacity of 3580 mAh/g and is a promising material to replace graphite (capacity 372 mAh/g), which is commonly used in anodes in present-day LIBs. However, Si undergoes large volume changes during lithiation/delithiation cycles, which results in its pulverization and loss of contact of active material with the current collector, leading to rapid capacity fading. Large volume changes of the Si is also thought to contribute to continuous mechanical degradation of the solid electrolyte interphase (SEI) layer, exposing fresh Si and continued formation of the SEI, contributing to capacity fading and poor Coulombic efficiency.[1−7]

Various approaches to improve cycling performance and reduce capacity fading have been reported. These include the use of alternate electrolytes that can form more stable SEI layers[8,9] and conductive binders that enhance the electrical conductivity of the anode.[10,11] Different Si architectures including nanowires,[12,13] nanotubes,[14,15] and nanospheres have been used, primarily designed to minimize the effects of large volume changes in Si.[6] Combinations of Si with various forms of carbon, such as graphite,[16,17] carbon black,[18] or graphene,[19] have been reported. The increased anode conductivity provided by carbon reduces capacity fading. In some architectures, the carbon loosely encapsulates the Si.[6] The void space around the Si accommodates its expansion during lithiation, alleviating stress related fracture of the surrounding conducting carbon.[20] Because carbon has a high conductivity, these anodes maintain good electrical contact with the current collectors over multiple charge/discharge cycles. Good conductivity and low contact resistance also promote efficient lithiation and delithiation.[21] Mechanical ball milling is the most common method reported for preparing uniform Si/C mixtures for anodes.[22,23] Thermal or chemical vapor deposition has also been used.[24−26]

In this paper, we report a new emulsion-templated directed assembly strategy to form Si/CB anodes that is simple to process and overcomes some of the major limitations restricting the use of Si-based anodes. We create an oil-in-water emulsion, with the oil droplets stabilized by conductive carbon black (CB) particles that are partially wetted by oil and water, and are fractal in structure. Excess CB particles form a connected network in the aqueous phase. The oil phase contains the Si nanoparticles. Upon drying this emulsion on a current collector, the Si particles remain confined within the regions previously occupied by oil. The CB particles occupying the

Received: November 5, 2013
Accepted: March 18, 2014
Published: March 18, 2014

  

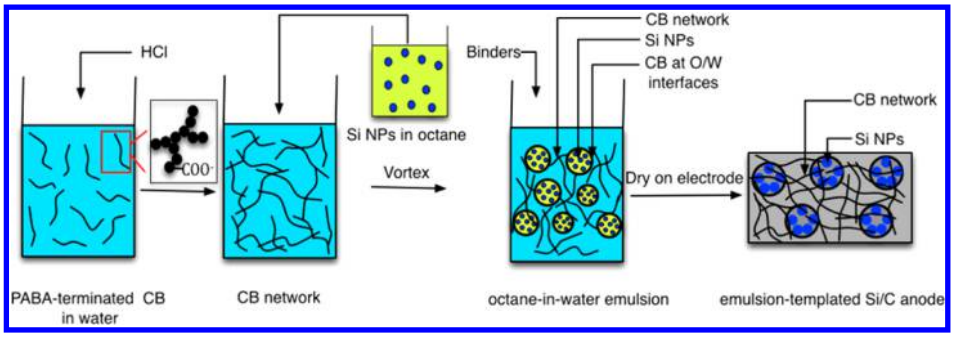


**Figure 1.** Schematic illustration of the emulsion-templated directed assembly method to prepare Si/CB anodes.

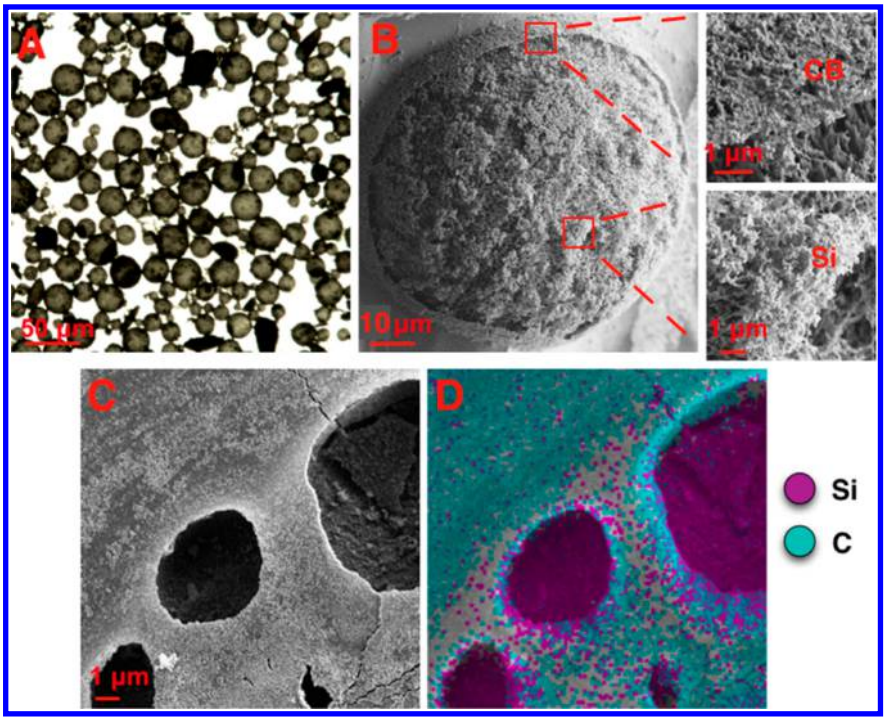


**Figure 2.** (A) A light microscope image of the Si/CB emulsion (diluted 10X with water). (B) A cryo-SEM image of the Si/CB emulsion. The magnified areas shown in the panels show CB and Si, respectively. (C) A FE-SEM image of the Si/CB electrode after drying the emulsion. (D) An EDS based elemental map of Si and C in (C). Most of the Si nanoparticles are in the regions previously occupied by octane, while the carbon is mostly confined to outside the Si-rich regions.

drop interfaces form a loosely bound mesoporous cage around the Si particles, while the CB that was in the water forms a conducting network around these carbon cages. The pore size in the cages is a function of the primary particle size in the CB. When consolidated into a half cell, the CB network comes into intimate contact with the electrolyte, but the Si particles are partially protected. The cage has space to accommodate the volume expansion of the Si NPs during lithiation, which helps to minimize transmission of stresses to the surrounding conducting CB network. Therefore electrical contact between the anode material and the current collector is not attenuated during charge/discharge cycles. The use of the emulsion template thus directs Si and CB particles into specific separated regions, desirable for performance enhancement of Si/CB anodes. In comparison to anodes formed by mixing dry Si NP and CB and depositing on a current collector, or with only Si NPs on the current collector, these emulsion-templated anodes have higher capacity and maintain superior cycling stability. The results show that this directed assembly technique holds promise for the formation of the next generation anodes for Li ion batteries.

## 2. MATERIALS AND METHODS

**2.1. Preparation of the Si/CB Anode.** A para-aminobenzoic acid-terminated carbon black (CB) suspension in water at pH 7.5 (Cabot Corporation, MA) was used in this study. Every CB particle consists of about 10 primary particles, each of diameter 20 nm, fused into a fractal aggregate of nominal dimensions 120−150 nm. The CB particles have a specific surface area of ~200 $m^2/g$. The $pK_a$ of the acid is ~6.5. Thus, the carboxyl groups are deprotonated at pH 7.5. The carboxylate termination on the CB particles makes them highly hydrophilic and allows them to be suspended stably in water. Si nanoparticles (average diameter of 50 nm) were purchased from Alfa Aesar.

The technique used to prepare the Si/CB anode is shown in Figure 1. 1 N hydrochloric acid is added to a 1.5% w/w CB suspension to a final concentration of 0.01 N. Addition of the acid protonates some of the surface carboxylate groups on the CB and increases the hydrophobicity of the initially highly hydrophilic particles. This hydrophilic/hydrophobic balance allows CB particles to reside at the oil−water interfaces during the subsequent emulsification step. It also causes the CB to form a connected network in the aqueous phase.[27]


dx.doi.org/10.1021/am404947z | ACS Appl. Mater. Interfaces 2014, 6, 4678−4683

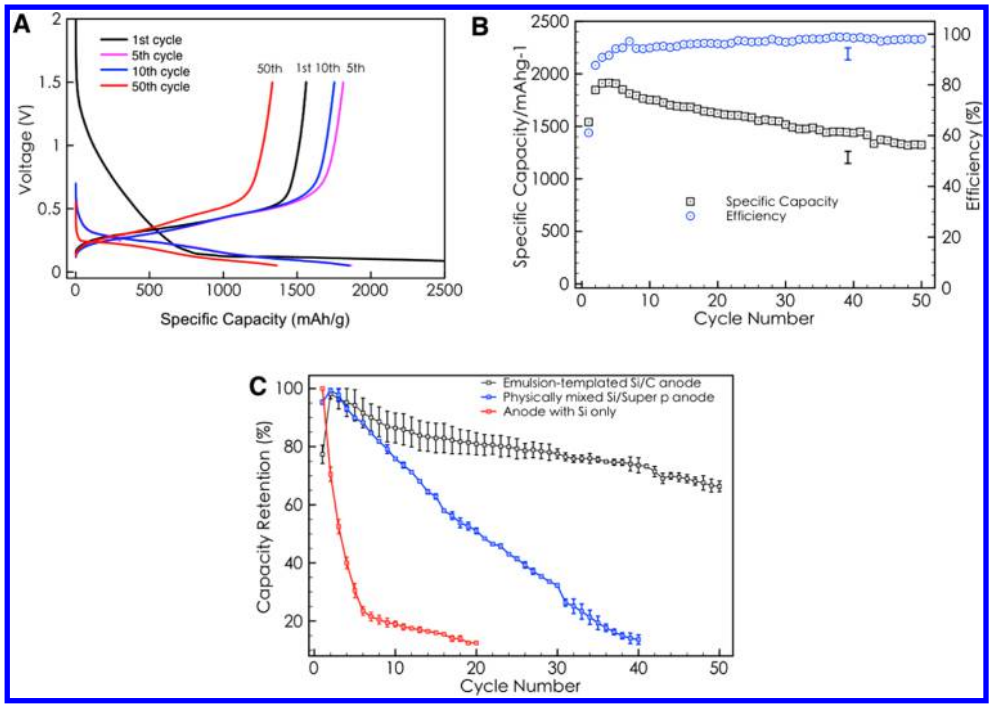


**Figure 3.** Electrochemical characterization of anodes. (A) Voltage profile for the emulsion-templated Si/CB anode during lithiation and delitiation. (B) Delithiation capacity and Coulombic efficiency of emulsion-templated Si/CB anode at a rate of C/10 (current of 1 mA/cm$^2$). The plots represent the average from three emulsion templated anodes; the two error bars indicate the maximum spread in the data. (C) Comparison of the delithiation capacity retention of different anodes, normalized by the maximum capacity. The plots are average values, and the error bars indicate the data spread, from three samples for each type of anode. The difference in performance between these anodes is statistically significant.

A 2.5% w/w suspension of Si nanoparticles in octane is mixed with the CB suspension at a ratio of 3:5 by volume. The ratio of the weights of Si nanoparticles to CB is 1:1. An aqueous solution of the binders carboxymethyl cellulose (CMC) and polyvinyl alcohol (PVA)[10,28] at a mass ratio of 1:1 is then added to the emulsion. The volume of the CMC/PVA solution is adjusted so that the final weight of binder after drying is 10% of the total anode mass (Si + CB + binder). After another 10 min of vortexing, 0.5 mL of the emulsion is placed on a stainless steel coin cell and dried overnight in an oven at 50 °C. This gentle and uniform drying process, the elastic modulus of the CB network and the presence of the binder, minimizes cracking caused by differential or rapid shrinkage of emulsion.[29]

Two other 'control' anodes, labeled Si/Super P and Si only, were prepared by forming a slurry of the dry (mixed in the case of Si/Super P) powder in water containing the binder and then sonicating this slurry for 30 min. 0.5 mL of the slurry is deposited on a stainless steel coin cell and dried in a vacuum oven at 50 °C. The Si concentration, the Si/CB ratio, and the binder concentration are maintained at the same values for all anodes.

**2.2. Cell Fabrication and Anode Electrochemical Characterization.** CR2032 type coin cells were assembled with specially designed current collector anodes and a lithium metal counter electrode. The anode loading was maintained at ~0.6 mg/cm$^2$, for all samples, and the coated layer thickness was ~100 $\mu$m. The electrolyte was 1.2 M $LiPF_6$ in a mixture of fluoroethylene carbonate (FEC)/ethylmethyl carbonate (EMC) at a ratio of 3:7 v/v. Both electrolytes were obtained from BASF. All samples were prepared in an Ar-filled glovebox with water vapor content at less than 1 ppm. An Arbin BT2000 was used for the cycling test. All half cells were subjected to galvanostatic (constant current) charge/discharge cycles with a cycling time of 10 h (C/10, current density of 1 mA/cm$^2$) from 0.05 V to 1.5 V versus Li/Li$^+$ at 25 °C.

**2.3. Characterization.** The Si/CB emulsion was observed by bright-field optical microscopy in a Nikon Eclipse E 600 microscope (the sample for optical microscopy was diluted to allow adequate transmittance) and by cryogenic scanning electron microscopy (cryo-SEM) using a Gatan Alto 2500 cryo station attached to a Zeiss Sigma FE-SEM. An uncycled emulsion-templated Si/CB anode was observed by SEM and selected area energy dispersive spectroscopy (EDS) in order to examine the spatial distribution of Si and CB. After cycling, the cells were disassembled in an argon-filled glovebox, and the electrodes were stored in an argon-filled vial. The electrodes were then observed using SEM. Delithiated electrodes after 50 cycles were also characterized using a JEOL 2100 transmission electron microscope. For observation using the TEM, we took a small piece of the electrode and dispersed it in dimethyl carbonate. A drop of the dispersion was then placed on a TEM grid and dried in a vacuum oven. The grid was stored in an argon-filled vial until it was observed. Samples were loaded rapidly into the TEM to minimize ambient exposure.

## 3. RESULTS AND DISCUSSION

Figure 2A is an optical microscope image showing O/W emulsions, with an average oil droplet size, measured using image J software of 100 drops, of ~20 $\mu$m.[30] We confirmed that this was an oil-in-water emulsion by adding a drop of water and a drop of octane to the emulsion. The water spread immediately, while the octane remained as a Si on the surface. A cryo-SEM image of a droplet is shown in Figure 2B. The porous CB cage surrounding the drop and the SI nanoparticles in the oil are shown in the magnified images.

As a rough estimate, each 20 $\mu$m octane droplet contains on average 5 × 10$^4$ NP. Thus nearly 99% of the volume inside the emulsion drop is unoccupied. The dimensions of the region occupied by the Si NP drops change by roughly a factor of 3 after drying, still leaving adequate space for Si expansion during lithiation. We note that this method of forming emulsions cannot guarantee that each oil droplet will have the same size or contain the same number of nanoparticles. This is a stochastic process that depends upon the mixing conditions. After drying at 50 °C in an oven and examining this sample using FE-SEM, the droplet morphology is visible (Figure 2C). Elemental

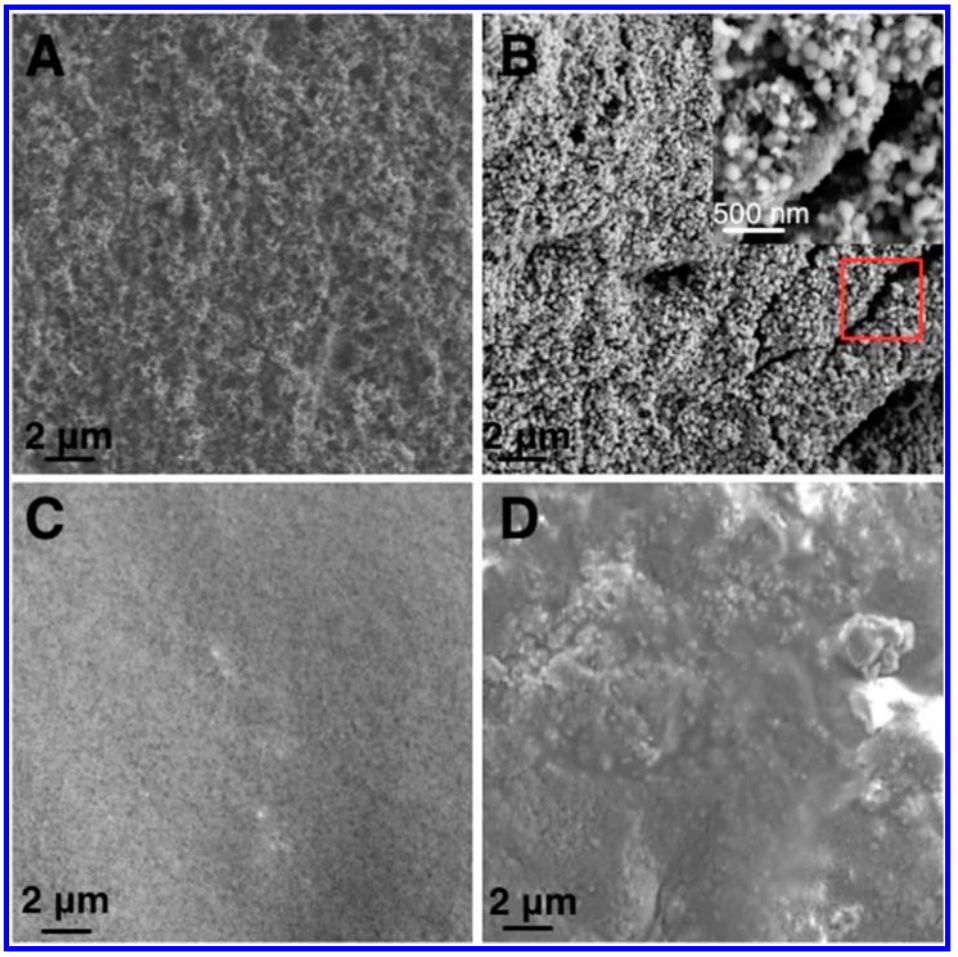


**Figure 4.** FE-SEM image of (A) fresh physically mixed Si/Super P anode. (B) The surface of the anode A after 50 cycles. The inset shows a magnified image of the region outlined. The Si NP are of the order of 100 nm, considerably expanded from their original size of 50 nm. (C) Fresh emulsion-templated Si/CB anode. (D) Emulsion-templated anode after 50 cycles.

mapping using EDS, shown in Figure 2D, confirms that the Si nanoparticles are confined to the 'oil' regions, and the CB particles surround these patches of Si nanoparticles.

The electrochemical cycling performance of the cells is shown in Figure 3. Figure 3A shows voltage versus capacity (all capacities are calculated based on the combined mass of Si and CB) for the Si/CB half cells at the first, fifth, 10th, and 50th cycle in the range 0.05 V to 1.5 V vs $Li/Li^+$. The plateau in the first cycle occurs at 0.18 V, indicative of lithiation of crystalline Si. The fifth and 10th cycles display higher capacity and good charge/discharge reversibility, showing that Si lithiation is more complete, and a stable SEI had formed, by the fifth cycle. Figure 3B shows that the Coulombic efficiency and delithiation capacity during the first cycle are low, about 55% and ~1540 mAh/g, respectively. The low first cycle efficiency is associated with SEI formation around the CB particles, promoted by their high specific surface area, as well as SEI formation around the Si NP.[31] The delithiation capacity increased to a maximum 1940 mAh/g after five cycles, indicating that most of the Si NPs have been activated by the fifth cycle. The delithiation capacity is ~1300 mAh/g after 50 cycles. The Coulombic efficiency varied between 95% and 99% and was at 97.4% at the end of the 50th cycle. We note that at lower cycle rates, Si lithiation can be much more complete at the end of the first charging cycle. The capacity will then show a drop over the following cycles. Figure 3C shows capacity retention, normalized by the maximum capacity, for anodes prepared using different techniques. The emulsion-templated Si/CB anode has only slight fading after 50 cycles. The void spaces in the conductive carbon cages permit Si NP expansion and contraction without transmitting excessive stresses on the surrounding CB network, allowing the electrically conducting pathway to the current collector to be maintained. However, the bare Si anode without conductive carbon and the physically mixed Si/Super P anode show rapid fading due to attenuated electrical contact between the anode material and the current collector as the Si NPs undergo volume changes during cycling.

The surfaces of the anodes before and after cycling are shown in Figure 4. Both the fresh Si/Super P physically mixed anode and the fresh emulsion-templated Si/CB anode look smooth with no obvious cracks (Figures 4A and 4C). After 50 cycles, many cracks formed on the surface of Si/Super P physically mixed anode (Figure 4B) indicating that the Si particles underwent extensive volume expansion and contraction, and these stresses were transmitted to the anode. The diameter of the Si NPs measured from the SEM images is ~100 nm, twice the original size, confirming the irreversible expansion of these particles at the end of 50 cycles. These volume changes lead to breaks of the SEI formed during the first lithiation, with concomitant exposure of fresh Si surfaces to the electrolyte, and additional SEI formation. Loss of active material, loss of electronic contact with the electrode, and persistent formation

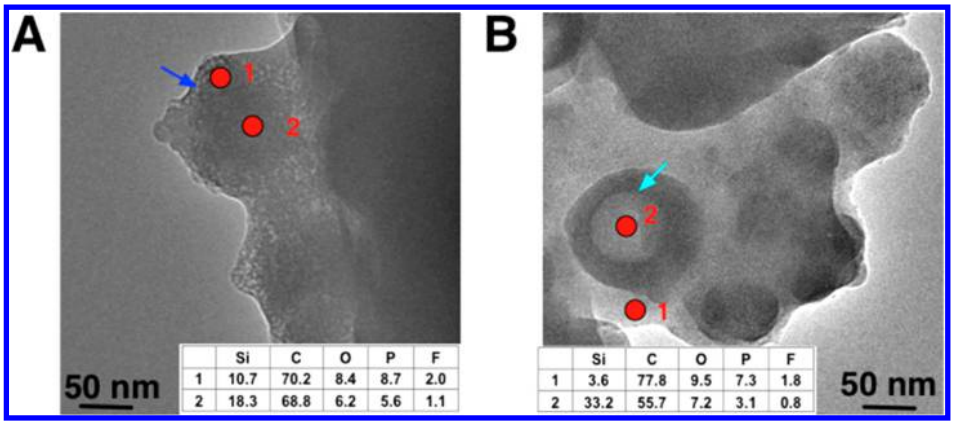


**Figure 5.** TEM images of (A) physically mixed Si/Super P anode. (B) Emulsion-templated Si/CB anode. The insets show the elemental compositions from selected areas. The dark blue arrow indicates a small piece of Si and a light blue arrow indicates the whole Si NPs.

of new SEI are partly responsible for the capacity fade in the Si/Super P anode.

No surface cracks and no pulverization of the Si nanoparticles were observed in the emulsion-templated Si/CB anode after 50 cycles (Figure 4D). This result is consistent with the electrochemical performance. Two important advantages of the Si/CB emulsion method improved the electrochemical performance and reduced the pulverization. Since many of the silicon NPs are encapsulated by a carbon black 'shell', they are more protected from the electrolyte, and much of the SEI was formed on the CB. This SEI remains stable during the cycling. Additionally, the protective carbon black cage around the Si NP allows expansion of the Si without significant breakage of electronic contact with the current collector. We suggest that these features are responsible for the slower capacity fade in the emulsion template anode.

Figure 5 shows the morphology of Si NPs after cycling. As shown in Figure 5A, the Si NP in the Si/Super P anodes suffered severe pulverization, and lost their distinctive spherical morphology. EDS data showed a significant amount of elemental Si in the SEI layer, comparable to the Si content away from it, suggesting that some small pieces of Si broke away and remained in the SEI when Si NPs shrank during delithation. For the emulsion-templated Si/CB anodes, the spherical shape of Si NPs was retained, as shown in Figure 5B. Compared to the center of Si NP, very little Si was detected around the particles, implying that Si NPs did not suffer severe pulverization.

The capacity, capacity retention, and Coulombic efficiency of our technique (not optimized) does not meet all of the performance metrics achieved by some of the other laboratory-based methods for forming Si/C anodes.[32,6,14,13,17] The key advance in our work is the low cost, simple method for preparing anodes, with Si and carbon spatially organized to accommodate volume changes in silicon while still maintaining good electrical contact with the current collector.

## 4. CONCLUSIONS

We report a simple emulsion-templated directed assembly technique for forming silicon carbon composite anodes for lithium ion batteries. Using this method, we are able to confine the Si nanoparticles to regions that are surrounded by a porous carbon black cage and an interconnected conductive carbon black network. The excess volume available within the cage accommodates much of the volume changes associated with the Si particles during lithiation and delithiation, minimizing stress propagation into the conducting network. Any transmitted stresses are absorbed by the elasticity of the network. Thus, electronic contact with the current collector is maintained throughout the lithiation and delithiation cycles. A stable solid electrolyte interphase appears to form around the high surface area CB particles. The use of Si NPs in a configuration that partially protects it from the electrolyte and the sustained electronic contact of the anode material with the current collector allows this anode to have a high capacity and good cycling performance after 50 cycles.

## AUTHOR INFORMATION

### Corresponding Authors

*E-mail: bosea@egr.uri.edu (A.B.).
*E-mail: cheny@egr.uri.edu (Y.C.).

### Notes

The authors declare no competing financial interest.

## ACKNOWLEDGMENTS

We gratefully acknowledge funding from Department of Energy Office of Basic Energy Sciences EPSCoR Implementation award (DE-SC0007074).

## REFERENCES

(1) Shi, H.; Barker, J.; Saidi, M. Y.; Koksbang, R.; Morris, L. Graphite Structure and Lithium Intercalation. *J. Power Sources* **1997**, *68* (2), 291−295.

(2) Tarascon, J. M.; Armand, M. Issues and Challenges Facing Rechargeable Lithium Batteries. *Nature* **2001**, *414* (6861), 359−367.

(3) Hatchard, T. D.; Dahn, H. R. In Situ XRD and Electrochemical Study of the Reaction of Lithium with Amorphous Silicon. *J. Electrochem. Soc.* **2004**, *151* (6), A838−A842.

(4) Xie, J.; Yang, X. G.; Zhou, S.; Wang, D. W. Comparing One- and Two-Dimensional Heteronanostructures As Silicon-Based Lithium Ion Battery Anode Materials. *ACS Nano* **2011**, *5* (11), 9225−9231.

(5) Key, B.; Bhattacharyya, R.; Morcrette, M.; Seznec, V.; Tarascon, J. M.; Grey, C. P. Real-Time NMR Investigations of Structural Changes in Silicon Electrodes for Lithium-Ion Batteries. *J. Am. Chem. Soc.* **2009**, *131* (26), 9239−9249.

(6) Wu, H.; Zheng, G. Y.; Liu, N. A.; Carney, T. J.; Yang, Y.; Cui, Y. Engineering Empty Space between Si Nanoparticles for Lithium-Ion Battery Anodes. *Nano Lett.* **2012**, *12* (2), 904−909.

(7) Nie, M.; Abraham, D. P.; Chen, Y.; Bose, A.; Lucht, B. L. Silicon Solid Electrolyte Interphase (SEI) of Lithium Ion Battery Characterized by Microscopy and Spectroscopy. *J. Phys. Chem. C* **2013**, *117* (26), 13403−13412.

(8) Chen, L. B.; Wang, K.; Xie, X. H.; Xie, J. Y. Effect of Vinylene Carbonate (VC) as Electrolyte Additive on Electrochemical Performance of Si Film Anode for Lithium Ion Batteries. *J. Power Sources* **2007**, *174* (2), 538−543.
(9) Dalavi, S.; Guduru, P. R.; Lucht, B. L. Performance Enhancing Electrolyte Additives for Lithium Ion Batteries with Silicon Anodes. *J. Electrochem. Soc.* **2011**, *159* (5), A642−A646.
(10) Magasinski, A.; Zdyrko, B.; Kovalenko, I.; Hertzberg, B.; Burtovyy, R.; Huebner, C. F.; Fuller, T. F.; Luzinov, I.; Yushin, G. Toward Efficient Binders for Li-Ion Battery Si-Based Anodes: Polyacrylic Acid. *ACS Appl. Mater. Interfaces* **2010**, *2* (11), 3004−3010.
(11) Choi, N. S.; Yew, K. H.; Choi, W. U.; Kim, S. S. Enhanced Electrochemical Properties of a Si-Based Anode Using an Electrochemically Active Polyamide Imide Binder. *J. Power Sources* **2008**, *177* (2), 590−594.
(12) Lin, L. H.; Sun, X. Z.; Tao, R.; Li, Z. C.; Feng, J. Y.; Zhang, Z. J. Photoluminescence Origins of the Porous Silicon Nanowire Arrays. *J. Appl. Phys.* **2011**, *110* (7).
(13) Cui, L.; Yang, Y.; Hsu, C.; Cui, Y. Carbon−Silicon Core−Shell Nanowires as High Capacity Electrode for Lithium Ion Batteries. *Nano Lett.* **2009**, *9* (9), 3370−3374.
(14) Cui, L. F.; Hu, L. B.; Choi, J. W.; Cui, Y. Light-Weight Free-Standing Carbon Nanotube-Silicon Films for Anodes of Lithium Ion Batteries. *ACS Nano* **2010**, *4* (7), 3671−3678.
(15) Park, M.-H.; Kim, M. G.; Joo, J.; Kim, K.; Kim, J.; Ahn, S.; Cui, Y.; Cho, J. Silicon Nanotube Battery Anodes. *Nano Lett.* **2009**, *9* (11), 689−798.
(16) Ng, S. H.; Wang, J. Z.; Wexler, D.; Konstantinov, K.; Guo, Z. P.; Liu, H. K. Highly Reversible Lithium Storage In Spheroidal Carbon-Coated Silicon Nanocomposites As Anodes For Lithium-Ion Batteries. *Angew. Chem., Int. Ed.* **2006**, *45* (41), 6896−6899.
(17) Zhou, W. C.; Upreti, S.; Whittingham, M. S. Electrochemical Performance of Al-Si-Graphite Composite As Anode for Lithium-Ion Batteries. *Electrochem. Commun.* **2011**, *13* (2), 158−161.
(18) Li, H.; Huang, X.; Chen, L. B.; Wu, Z.; Liang, Y. A High Capacity Nano - Si Composite Anode Material for Lithium Rechargeable Batteries. *Electrochem. Solid-State Lett.* **1999**, *2* (22), 547−549.
(19) He, Y. S.; Gao, P. F.; Chen, J.; Yang, X. W.; Liao, X. Z.; Yang, J.; Ma, Z. F. A Novel Bath Lily-Like Graphene Sheet-Wrapped Nano-Si Composite As a High Performance Anode Material for Li-Ion Batteries. *RSC Adv.* **2011**, *1* (6), 958−960.
(20) Ng, S. H.; Wang, J.; Wexler, D.; Konstantinov, K.; Guo, Z. P.; Liu, H. K. Highly Reversible Lithium Storage in Spheroidal Carbon-Coated Silicon Nanocomposites As Anodes for Lithium-Ion Batteries. *Angew. Chem., Int. Ed. Engl.* **2006**, *45* (41), 6896−9.
(21) Terranova, M. L.; Orlanducci, S.; Tamburri, E.; Guglielmotti, V.; Rossi, M. Si/C Hybrid Nanostructures for Li-Ion Anodes: An Overview. *J. Power Sources* **2014**, *246* (15), 167−177.
(22) Kasavajjula, U.; Wang, C. S.; Appleby, A. J. Nano- and Bulk-Silicon-Based Insertion Anodes for Lithium-Ion Secondary Cells. *J. Power Sources* **2007**, *163* (2), 1003−1039.
(23) Wang, P.; NuLi, Y.; Yang, J.; Zheng, Y. Carbon-Coated Si-Cu/Graphite Composite as Anode Material for Lithium-Ion Batteries. *Int. J. Electrochem. Sci.* **2006**, *1* (3), 122−129.
(24) Yoshio, M.; Wang, H.; Fukuda, K.; Umeno, T.; Dimov, N.; Ogumi, Z. Carbon-Coated Si as a Lithium-Ion Battery Anode Material. *J. Electrochem. Soc.* **2002**, *149* (12), A1598−A1603.
(25) Kong, J. H.; Yee, W. A.; Wei, Y. F.; Yang, L. P.; Ang, J. M.; Phua, S. L.; Wong, S. Y.; Zhou, R.; Dong, Y. L.; Li, X.; Lu, X. H. Silicon Nanoparticles Encapsulated in Hollow Graphitized Carbon Nanofibers For Lithium Ion Battery Anodes. *Nanoscale* **2013**, *5* (7), 2967−2973.
(26) Holzapfel, M.; Buqa, H.; Krumeich, F.; Novak, P.; Petrat, F.; Veit, C. Chemical Vapor Deposited Silicon/Graphite Compound Material as Negative Electrode for Lithium-Ion Batteries. *Electrochem. Solid-State Lett.* **2005**, *8* (10), A516−A520.
(27) Saha, A.; Nikova, A.; Venkataraman, P.; John, V. T.; Bose, A. Oil Emulsification Using Surface-Tunable Carbon Black Particles. *ACS Appl. Mater. Interfaces* **2013**, *5*, 3094−3100.
(28) Guo, Z. P.; Jia, D. Z.; Yuan, L.; Liu, H. K. Optimizing Synthesis Of Silicon/Disordered Carbon Composites for Use As Anode Materials In Lithium-Ion Batteries. *J. Power Sources* **2006**, *159* (1), 332−335.
(29) Feng, H. H.; Sprakel, J.; Ershov, D.; Krebs, T.; Stuart, M. A. C.; van der Gucht, J. Two Modes of Phase Inversion in a Drying Emulsion. *Soft Matter* **2013**, *9* (10), 2810−2815.
(30) Abramoff, M. D.; Magalhães, P. J.; Ram, S. J. Image Processing with ImageJ. *Biophotonics Int.* **2004**, *11* (7), 36−42.
(31) Chung, G. C.; Jun, S. H.; Lee, K. Y.; Kim, M. H. Effect of Surface Structure on the Irreversible Capacity of Various Graphitic Carbon Electrodes. *J. Electrochem. Soc.* **1999**, *146* (5), 1664−1671.
(32) Jung, D. S.; Hwang, T. H.; Park, S. B.; Choi, J. K. Spray Drying Method for Large-Scale and High-Performance Silicon Negative Electrodes in Li-Ion Batteries. *Nano Lett.* **2013**, *13* (5), 2092−2097.